Numerical study on prestressed concrete containment building: creep, ageing and leakage. Application to VERCORS mockup

Try Meng, Ludovic Jason, Thomas Heitz, Benjamin Richard

▶ To cite this version:

NUMERICAL STUDY ON PRESTRESSED CONCRETE CONTAINMENT BUILDING: CREEP, AGEING AND LEAKAGE. APPLICATION TO VERCORS MOCKUP

Try Meng[1,*], Ludovic Jason[1], Thomas Heitz[2] and Benjamin Richard[2]

[1] Université Paris-Saclay, CEA, Service d'Etude Mécaniques et Thermiques, 91191, Gif-sur-Yvette, France. *Corresponding author (try.meng@cea.fr)
[2] IRSN, SES, LMAPS, Fontenay aux Roses F-92260, France.

ABSTRACT

The containment building (CB) is known as the third and last safety barrier to protect the environment from diffusion of radioactive products. In 2014, Électricité de France (EDF) launched the VERCORS project (J. Niepceron, 2021) to improve the knowledge of leak-tightness in the CB under air pressure loading and ageing effects. VERCORS consists in a 1/3 scaled containment mock-up representing a 1300 MWe CB of a typical French pressurized water reactor (PWR). The CB is well monitored by experimental approach, in parallel, international benchmarks have been proposed in order to compare different numerical simulations techniques. This paper presents the results of the simulation based on VERCORS mock-up, and the simulation includes early-age phase, prestress phase and pressurization phase. The finite element solver is performed by Castem (Castem, 2019). Concrete is modelled through 3D elements while rebar and tendons are modelled by 1D elements. The delayed strains including creep and shrinkage are calculated through the BPEL99 model (BPEL99, 1999). The effects of friction and relaxation on the prestress level are taken into account. Besides that, pressure load and ageing scenario are included. To describe cracks in concrete, an elastic damage model (Mazars, et al., 2015) is used for the concrete elements, and the post-processing of leak-tightness is based on the internal variable of the damage model and a hydraulic analysis. The mechanical results reveal different damage zones on the CB, which are distributed at gusset, hatch and dome. Under the constant relative pressure tests, the damage develops from the gusset to the wall, this is because of the increasing of prestress loss due to the delayed strains.

INTRODUCTION

In France, 70% of the electricity is powered by the nuclear power plant (NPP) and a precise study of the mechanical behaviour of the CB is essential to guarantee its functionality. VERCORS mock-up is constructed in prestressed reinforced concrete, and the reduction scale helps to shorten the drying process in concrete element, which is a key factor to accelerate aging effect in concrete. As a result, 1 year of observation in VERCORS mock-up is equivalent to 10 years in a full scale CB. About 700 sensors (thermometer, time domain reflectometry, flow meter…) and 2 km of optical fibre are embedded in concrete. The measured results cover from temperature, saturation degree, displacements, strains, crack opening to air leakage during the pressure tests. Hundreds of VERCORS concrete samples are tested for drying, shrinkage and creep effects, and are used to characterize mechanical parameters at different temperatures situations. Along with those results from VERCORS concrete, the simplified shrinkage and creep models used in the current simulation are validated. In this paper, the simulation aims at reproducing the experimental results by balancing between the complexities of the simulation and the accuracy of the results. Three principal phenomena are considered, they are early-age phase, prestress phase and pressurization phase (*Figure 1*).

26th International Conference on Structural Mechanics in Reactor Technology
Berlin/Potsdam, Germany, July 10-15, 2022
Division V *(Modelling, Testing & Response Analysis of Structures, Systems and components)*

The early-age phase is only simulated with the gusset, which is known as massive element of the CB. The simulation is a weak coupled thermal-hydro-mechanical analysis (THM), which means that there is no influence from mechanical results to thermal and hydraulic analyses. The gusset is poured at 34 days after the construction of raft foundation (t_0), thus the simulation starts at 34 days ($t_{early-age}$) until 278 days, when the construction of CB is finished. Before 34 days, no simulation is made since the gusset is not constructed. From 34 to 278 days, thermal strains (ε_{th}), shrinkage strains (ε_{sh}) and self-weight are included in the simulation. ε_{th} is calculated through the dilatation coefficient with temperature distribution, whereas the ε_{sh} is based on linear shrinkage model (Wittmann, et al., 1980) with water content distribution.

The simulation continues to the prestress phase with full VERCORS mock-up, and starts at 280 days, which is considered as the initial time step. At this time step, the prestress have not applied, but the initial ε_{sh} is calculated, and the results from the last time step of early-age phase in the gusset are input into this time step as the initial conditions. Those input results include damage variables, stresses, strains and displacements. Adding this initial time step also helps to activate the calculation of creep strain (ε_{creep}) in the next time step at 302 days, which is corresponding to the starting point of the prestress time step (302-380 days), see in *Table 1*. ε_{creep} is a stress dependent strain, thus ε_{creep} at 302 days is calculated from the stress state at 280 days. In the loop of prestress time step, prestress force, self-weight, ε_{sh} and ε_{creep} represent the external forces applied to the structure. Difference from early-age phase, ε_{sh} and ε_{creep} in prestress and pressurization phases are calculated through a simplified model, BPEL99 (BPEL99, 1999). This simplification have lightened the simulation since no thermal and hydraulic analyses are involved.

After ending prestress phase at 380 days, pressurization phase is carried on. The pressure scenario is adapted to the one provided by EDF. From VO1 to VD6, the relative pressure is fixed at 4.2 bar and is applied to the inner face of the CB, see in *Table 1*. In each pressure test, there are prestress, self-weigh, delayed strains and pressure load. The mechanical behaviour of the concrete in those three phases is elastic damage behaviour. The damage variable allows for estimating the crack opening, as well as, the post-processing of leakage through crack.
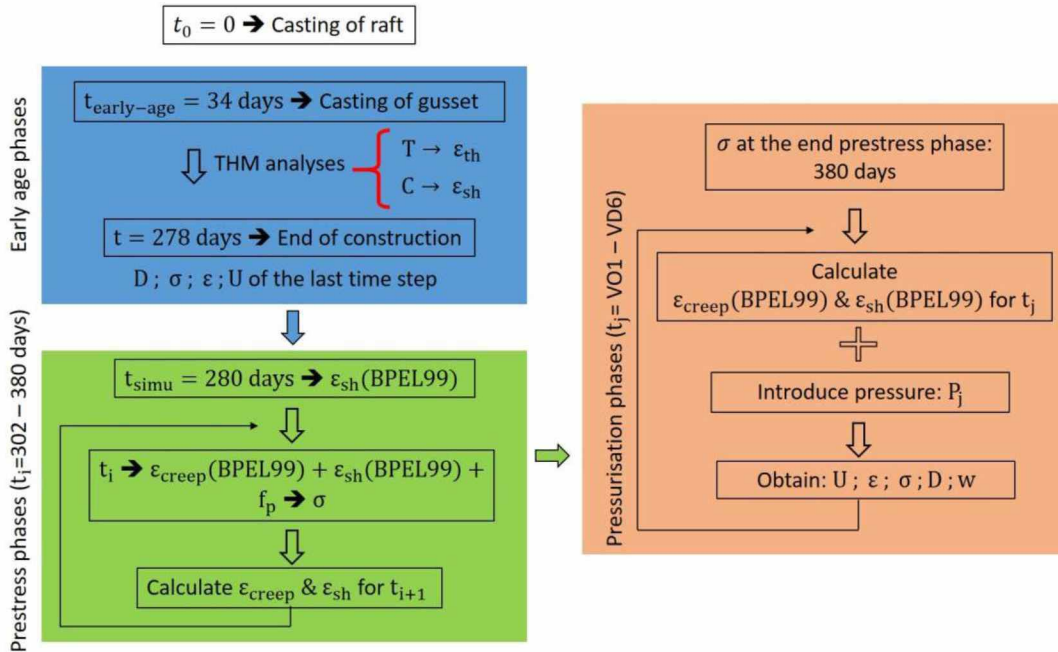

Figure 1: Summary steps of simulation

26th International Conference on Structural Mechanics in Reactor Technology
Berlin/Potsdam, Germany, July 10-15, 2022
Division V *(Modelling, Testing & Response Analysis of Structures, Systems and components)*

CONSTITUTIVE LAWS

Concrete & rebar

To describe cracks in concrete and the unilateral effect, the elastic damage μ-model (Mazars, et al., 2015) is used in the current simulation:

$$\sigma = (1 - D)\mathbf{E} : \varepsilon^e$$

Table 1: Prestress and pressurization phases

Prestress phase						Pressurization phase		
phase	day	CABV	CABH	CABG	CABD	Phase	Day	Notice
1	302	27	14	-	-	$t_{reference}$	24/07/2014: 0	Start construction
2	307	30	14	-	-	VO1	469	
3	316	-	26	18	2	VC1	551	
4	335	-	20	17	-	VD1	964	
5	340	-	18	34	-	VD1bis	971	4.2 bar
6	364	-	12	28	-	VD2	1344	
7	370	-	18	-	-	VD3	1699	
8	376	-	-	-	6	VD5	2403	
9	380	-	-	-	10	VD6	2806	

The parameters of the damage model and the VERCORS data are presented in *Table 2*, the stress-strain curve of a uni-axial test is illustrated in *Figure 2*. It should be noticed that the raft foundation is considered as a rigid element. For the rebar, a classic elasto-plastic model is applied, and the parameters are described in *Table 2*, the input stress-strain curve is plotted in *Figure 2*.

Table 2: VERCORS data and parameters of the models

concrete	VERCORS data: $\rho = 2395 kg/m^3$; E$_c$=34300 MPa; f$_c$=48.7 MPa ; f$_t$=4.4 MPa									
	Parameters of the model									
	E$_c$ (MPa)	υ	f$_t$ (MPa)	A$_t$	B$_t$	A$_c$	B$_c$	ε_{0t}	ε_{0c}	α
	34300	0.18	4.4	0.9	7795	1.4	390	1.28E-4	3E-4	1E-5

rebar	VERCORS data: E$_a$=200000MPa; maximum yield stress = 500MPa			
	E$_a$ (MPa)	υ	f$_e$ (MPa)	f$_y$ (MPa)
	200000	0.33	412	477

Tendon

Only the elastic behaviour is applied to the tendons, besides that, the instantaneous prestress loss related to the friction and wedge pull-in at anchorage is calculated through the BPEL99 (BPEL99, 1999). EDF provides the standard parameters of prestress loss with the standard of ETA-06/0226/system C (4C15), see in *Table 3*.
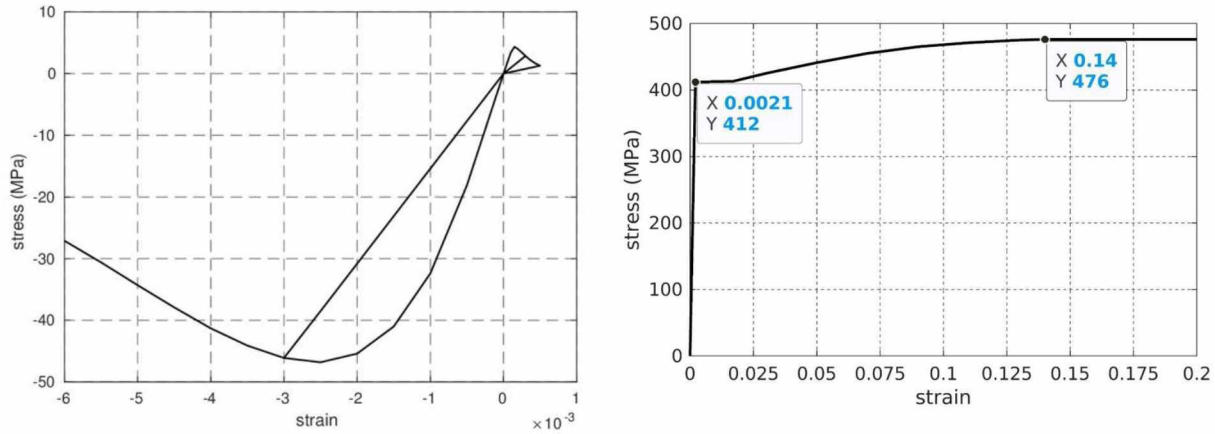
26th International Conference on Structural Mechanics in Reactor Technology
Berlin/Potsdam, Germany, July 10-15, 2022
Division V *(Modelling, Testing & Response Analysis of Structures, Systems and components)*

Figure 2: Stress-strain curve (left: concrete; right: rebar)

Table 3: Parameters for prestress loss and tendon

VERCORS data: E_p=190000MPa; v=0.33; A_s=556mm^2						
Parameters of prestress loss						
f (rd^{-1})	ϕ (m^{-1})	f_p (MPa)	ρ_{1000}	μ_0	l_{anchor} (m)	f_e (KN)
017	0.0015	1860	2.5%	0.43	0.008	827

NUMERICAL MODELLING & BOUNDARY CONDITIONS

The numerical model is based on the VERCORS mock-up, and is modelled in three dimensions. The concrete is modelled by solid elements, rebar and tendons are meshed with 1D elements, see in *Figure 3*. The maximum dimension of solid elements is fixed at 0.35m, and there are 158527 elements. The bottom surface of the raft foundation is blocked with all displacements, whereas the interface between rebar-concrete and tendon-concrete is made by perfectly rigid interface, rebar and tendon displace in the same way as those of the concrete elements.
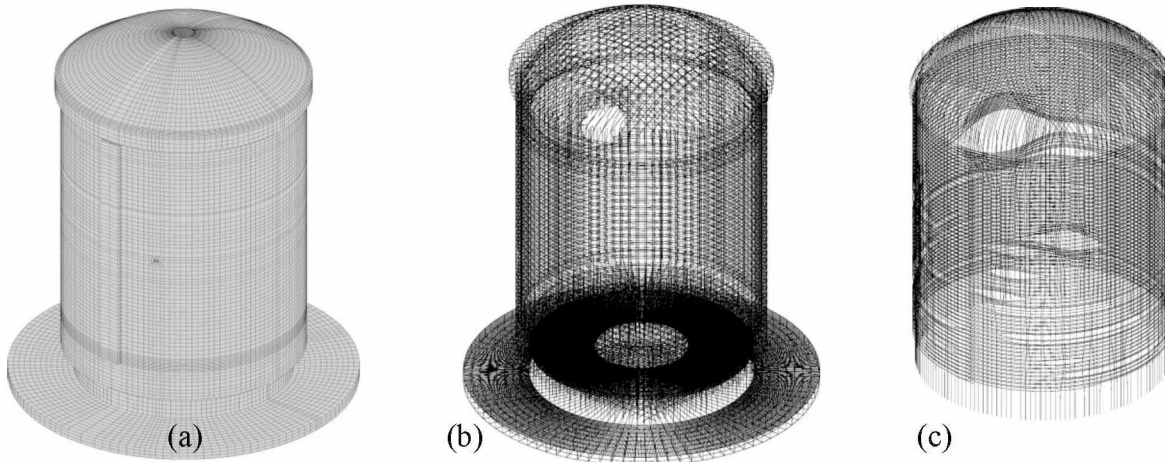

(a)   (b)   (c)

Figure 3: (a) Concrete; (b) Rebar; (c) Tendon

26th International Conference on Structural Mechanics in Reactor Technology
Berlin/Potsdam, Germany, July 10-15, 2022
Division V *(Modelling, Testing & Response Analysis of Structures, Systems and components)*

SHRINKAGE & CREEP VALIDATION

The shrinkage and creep models, which are used in prestress and pressurization phases, are based on the BPEL99 (BPEL99, 1999). Simulation tests are done and compared to the experimental results of VERCORS concrete. In *Figure 4*, the concrete samples of shrinkage and creep tests are exposed to 50% of relative humidity, and 12 MPa in compression is added to the creep test. The results of the simplified models on the delayed strains are provided in *Figure 5*.
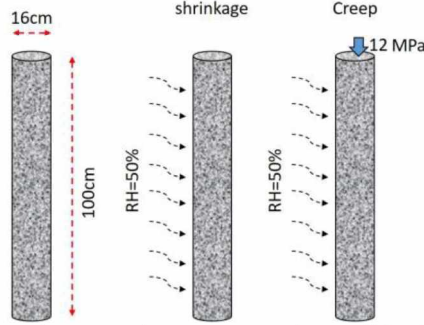

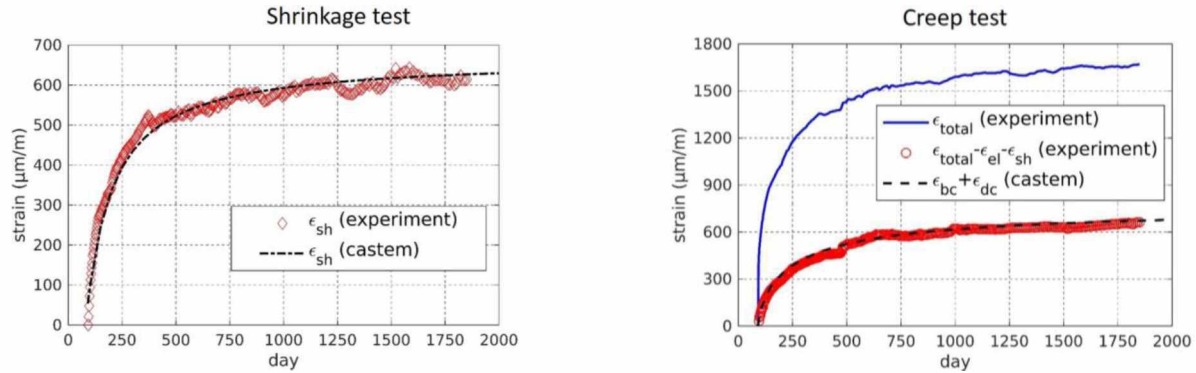*Figure 4: Shrinkage and creep test of VERCORS concrete*

Figure 5: Comparison of shrinkage and creep strains between experiment and simulation

THERMAL AND HYDRAULIC ANALYSES FOR EARLY-AGE PHASE

As mentioned in the introduction, only ε_{th} and ε_{sh} are included, thus classic thermal and hydraulic analyses are performed, see in *Figure 6*. The parameters of those analyses are summarized:
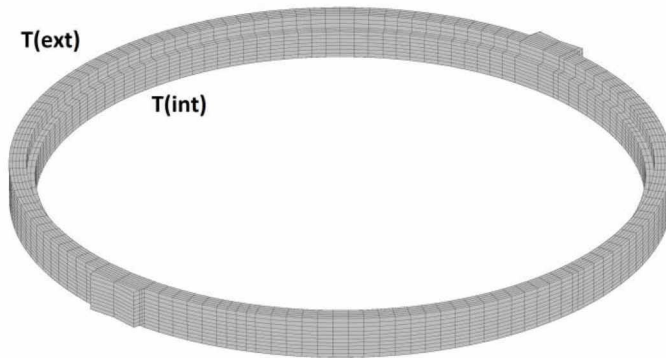
	Formwork	No formwork
λ	2.5 (w/m°C)	
ρ	2395 (kg/m^3)	
C_p	880 (J/kg°C)	
H_T	40 (W/m^2°C)	20 (W/m^2°C)
K^c_{sh}	7.1E-6 (m^3/l)	

$$\dot{\varepsilon}_{th} = \alpha \dot{T} I \quad ; \quad \dot{\varepsilon}_{sh} = K^c_{sh} \dot{C} I$$

Figure 6: Numerical modelling of the gusset

26th International Conference on Structural Mechanics in Reactor Technology
Berlin/Potsdam, Germany, July 10-15, 2022
Division V *(Modelling, Testing & Response Analysis of Structures, Systems and components)*

Figure 7 is the ambient temperature and water content evolutions that are applied to the outer and inner faces of the gusset. In particular, the gusset is initially heated up to 50°C (with formwork). Moreover, ε_{th} is calculated with a classic expression, but ε_{sh} is obtained through the linear shrinkage model (Wittmann, et al., 1980) (Bazant, et al., 1994).
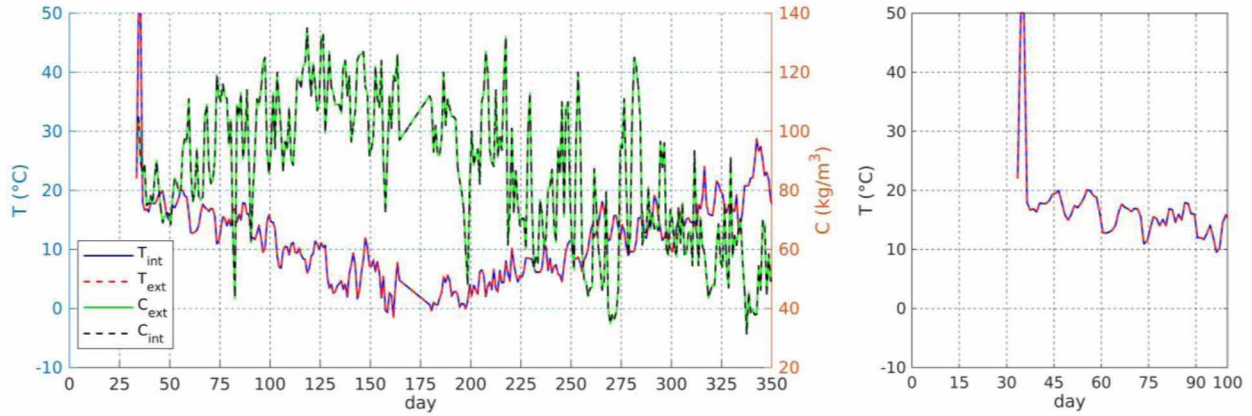

Figure 7: Imposed temperature water content evolution (EDF)
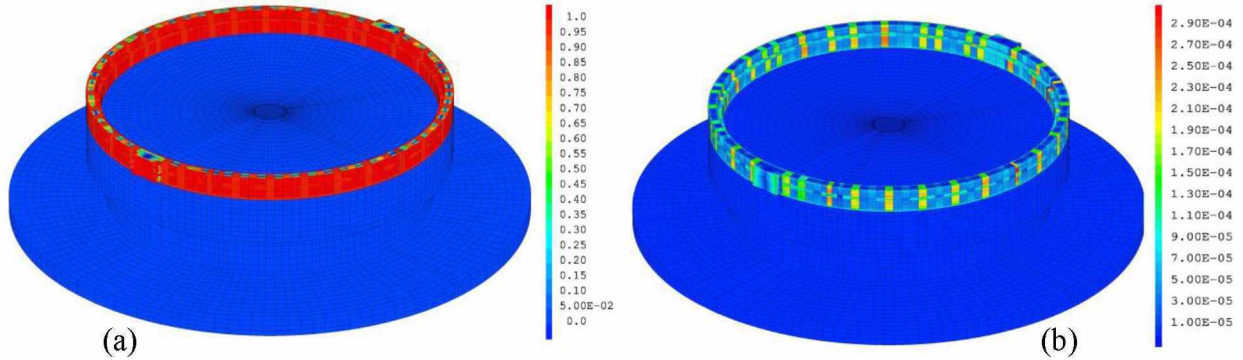
RESULTS

Early-age phase

Figure 8: (a) Damage distribution; (b) Crack opening (unit: m)

The damage and crack opening distribution in the gusset are illustrated in *Figure 8*. The damage uniformly distributes on the skin of the gusset, and several damages zones spread through the thickness. The crack opening is calculated from 'OUVFISS', which is a module originally implemented in Castem (Castem, 2019). This module is based on the formulation of (Matallah, et al., 2010), in which the crack opening is obtained from the difference stress between elastic stress (σ_e) and damage stress (σ (D)). The early-age phase detects several vertical cracks in the gusset, which confirm to the observation of vertical cracks from the experiment. Those vertical cracks in the gusset are potentially caused by the displacement constraints between the dilatation effect (heating) and contraction (shrinkage).

Prestress phase

In *Figure 9*, the crack opening distribution is presented, and a typical focus on the gusset is made. After tensioning the tendons, concrete pertains compression stress. In µ-model (Mazars, et al., 2015), the effective damage (D_{eff}) is combined from two thermodynamic variables 'Yt' (tensile strain) and 'Yc'(compression strain) through the driving variable Y. Thus in the gusset, stresses switched from tension to compression

26th International Conference on Structural Mechanics in Reactor Technology
Berlin/Potsdam, Germany, July 10-15, 2022
Division V *(Modelling, Testing & Response Analysis of Structures, Systems and components)*

make the reduction in Y_t, and since the compression stress is not large enough to activate Y_c, then the D_{eff} reduces and rigidity matrix recovers, eventually the displacements and strains decrease. As a result, the cracks opening in the gusset from the early-age phase are partially closed. From this, it should be mentioned that the choice of constitutive law in concrete must be considered the unilateral effect. Furthermore, no crack opening is observed numerically either on the wall or on the dome.
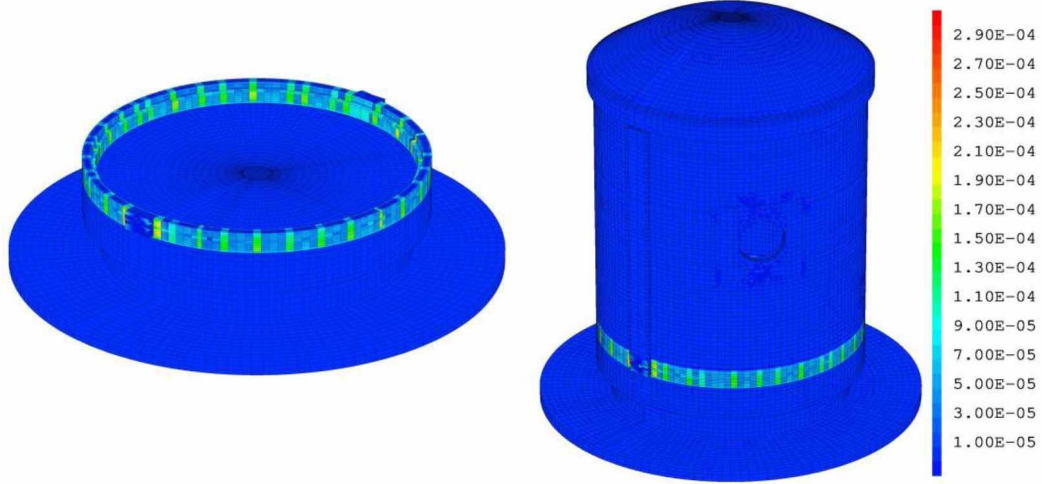

Figure 9: Crack opening distribution in full VERCORS mock-up at the end of prestress (unit: m)

Pressurization phase

In pressurization phase, the complete strains evolution in the wall are extracted in vertical and tangential directions, and are compared with the results of the experiment, see in *Figure 10*. As mentioned in the introduction, there is no early-age effect in the wall, thus from t=0 to t=278 days, there is no relevant result related to the wall. From t=280 to 380 days, the strains largely increase and this results from the prestressing in the tendons. At each pressure test, the negative strains reduce and the CB inflates. Globally, the strains continue to develop in time evolution, and this is caused by the delayed strains. The vertical strain matches with the result of the experiment, whereas it remains a difference to the measured tangential strain. The shifting in the tangential strain might be caused by the estimation of prestress loss in horizontal tendons. To confirm this assumption, an extra experimental prestressed force in the tendons is needed.
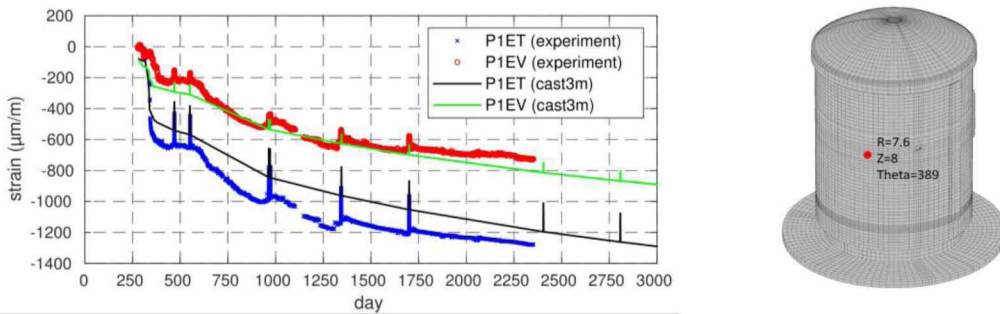

Figure 10: Comparison strains evolution

Besides strain evolutions, stress evolutions are extracted at the dome, wall and gusset, see in *Figure 11*. Due to the prestressing tendons, the compression stresses in the wall reach to 12 MPa and 6 MPa for tangential and vertical directions, respectively. The stresses reduce progressively in time evolution, and this is explained by the increasing in prestress loss due to the delayed strains.
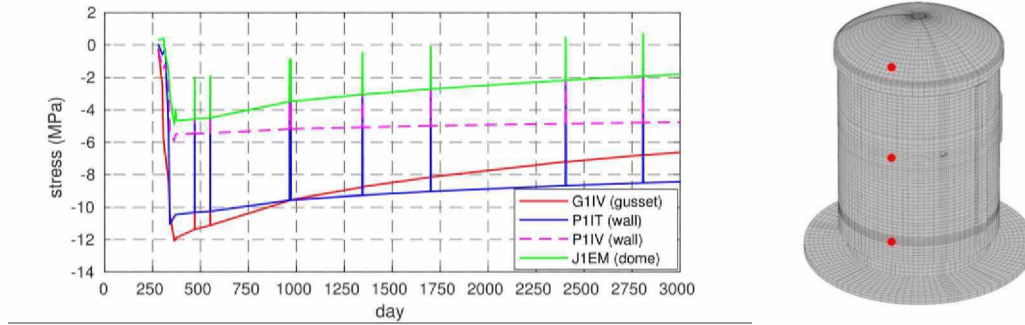
26th International Conference on Structural Mechanics in Reactor Technology
Berlin/Potsdam, Germany, July 10-15, 2022
Division V *(Modelling, Testing & Response Analysis of Structures, Systems and components)*

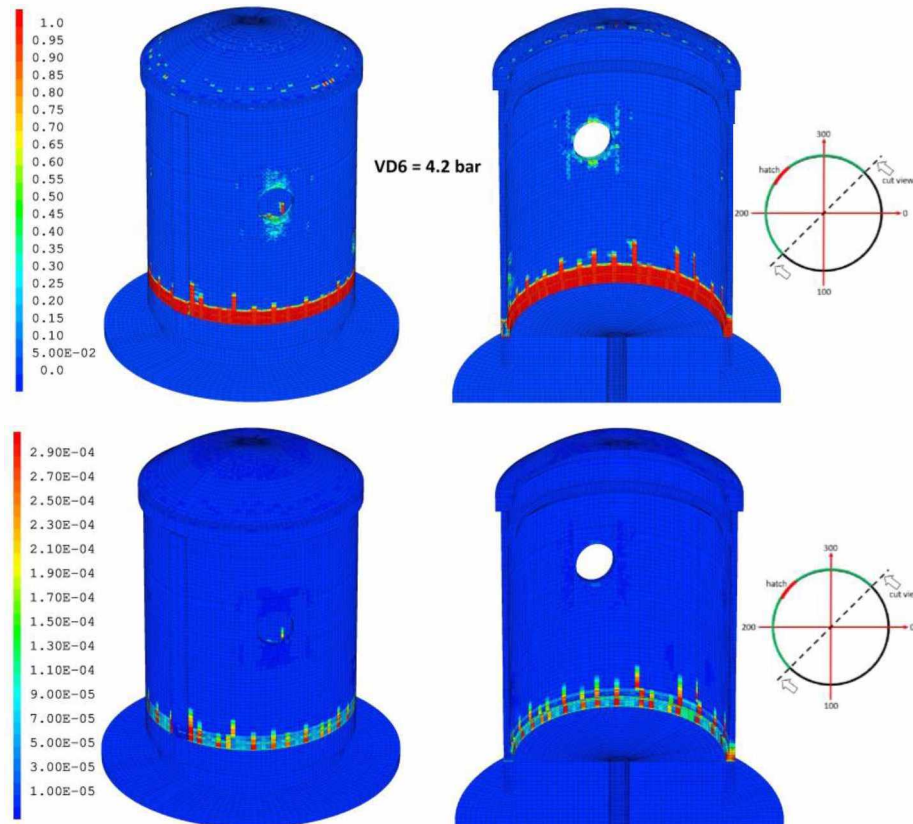*Figure 11: Stresses evolution*

Figure 12: Damage (top) & crack opening distribution (bottom, unit: m) at VD6
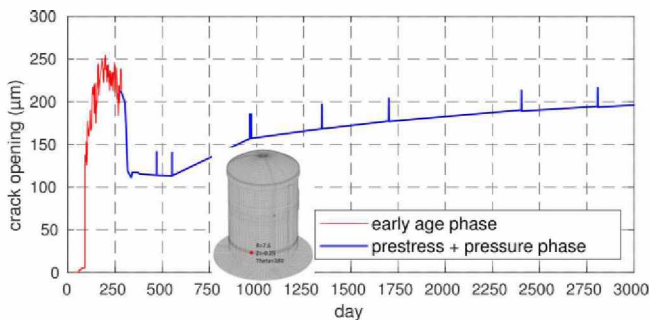
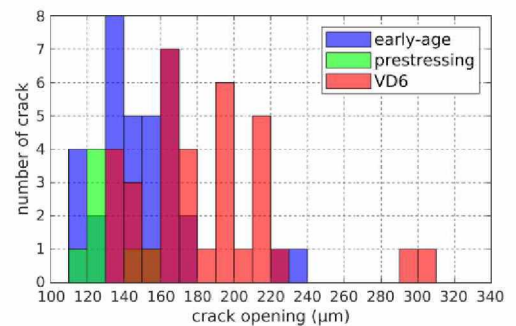*Figure 14: Crack opening evolution*

Figure 13: Histogram of crack opening

26th International Conference on Structural Mechanics in Reactor Technology
Berlin/Potsdam, Germany, July 10-15, 2022
Division V *(Modelling, Testing & Response Analysis of Structures, Systems and components)*

In *Figure 12*, the damage and crack opening distribution at VD6 (2806 days) are plotted, and the vertical cracks develop from the gusset to the wall. All pressure tests, VO1 to VD6, are set at 4.2 bar, and the supplemental cracks in the wall first appear during VD2 because of the increasing prestress loss in the tendons. Crack opening evolution is shown in *Figure 14*, in early-age phase, cracks spread in the gusset. Once switching to prestress phase, those cracks are partially closed, whereas they are re-opened during the pressure tests. The histogram of crack opening in *Figure 13* presents globally the number of cracking patterns that corresponds to each crack opening. In VD6, crack opening and number of cracks increase by comparing to those in the early-age and prestress phases.

LEAK-TIGHTNESS (Q_g)

Porosity leakage (Q_d)

The global flow rate (Q_g) is the sum of porosity leakage and local leakage through crack. The porosity leakage in this paper is based on the Darcy model. In this simplified configuration, only the drying air is considered. Limiting to the space, only the principal equations are presented, and the details of post-processing of porosity leakage is found in (Jason, et al., 2007). The calculation of Q_d is a function of the fluid velocity, V_5 that corresponds to the outer face of the CB is chosen, see in *Figure 15*.
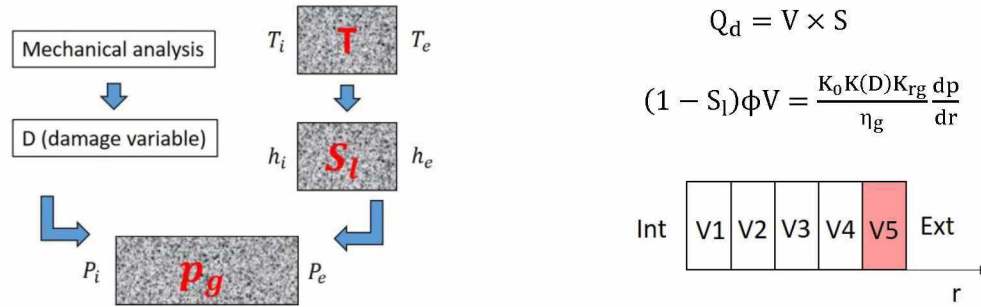

$$Q_d = V \times S$$

$$(1 - S_l)\phi V = \frac{K_0 K(D) K_{rg}}{\eta_g} \frac{dp}{dr}$$

Figure 15: Post-processing of porosity leakage

Local leakage through crack (Q_p)

The local flow rate is based on the Poiseuille model. Crack opening (W), crack length (L) and roughness of crack (ξ=0.01) are important parameters to calculate Q_p. The through crack opening at VO1 is illustrated in *Figure 16* as an example. In each cracking pattern, the average crack opening is calculated in two approaches: W_m = average W of all elements; $W_r = \sqrt[3]{1/i}$, in which i is mean value of $1/W^3$ (Jason, et al., 2014). Furthermore, L of each cracking pattern is obtained by counting the number of elements in vertical direction and multiplying with its dimension. It should be noticed that only cracking pattern with W_m or W_r > 100µm is taken into account, as prescribed by EDF for the benchmark, which is used to identify the experimental cracking patterns.
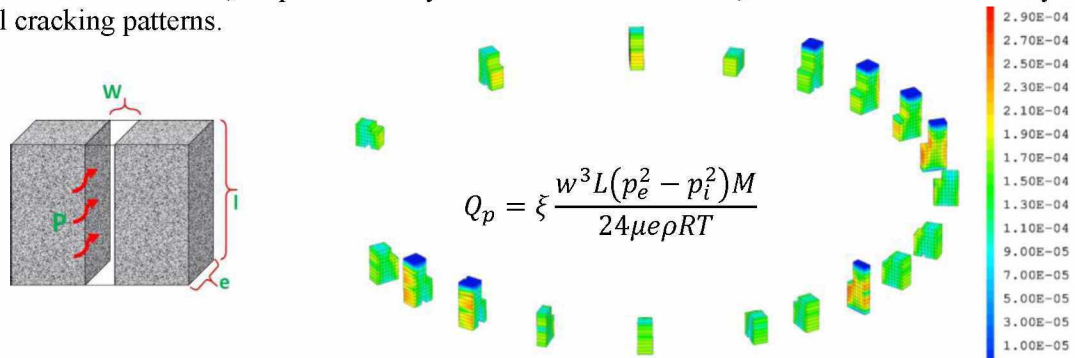

$$Q_p = \xi \frac{w^3 L (p_e^2 - p_i^2) M}{24 \mu e \rho R T}$$

Figure 16: Principal fluid flow through crack opening (unit: m) at VO1

26th International Conference on Structural Mechanics in Reactor Technology
Berlin/Potsdam, Germany, July 10-15, 2022
Division V *(Modelling, Testing & Response Analysis of Structures, Systems and components)*
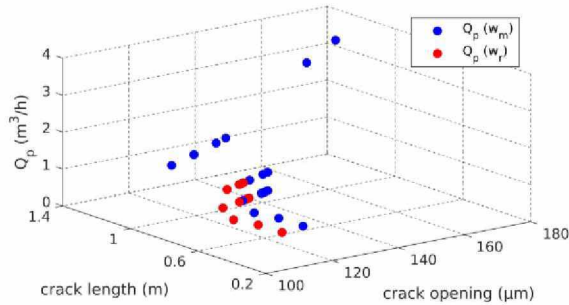

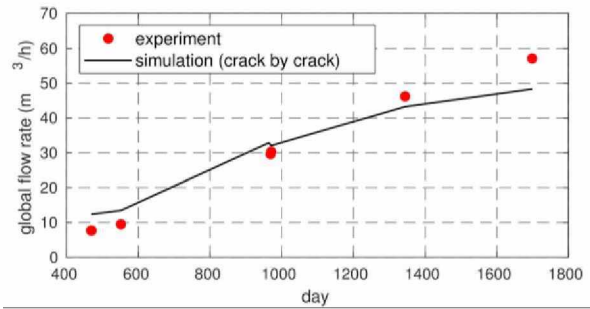*Figure 18: Q_p of each cracking pattern at VO1*

Figure 17: Global flow rate, $Q_g=Q_d+Q_p(W_r)$

The Q_p of each cracking pattern are calculated with different approaches of crack opening (W_m and W_r), see in *Figure 18*. Thus, the total $Q_{p,total}$ in each pressure tests is the sum of all Q_p from all cracking patterns, and $Q_p(W_m)$ estimates larger flow rate than those of $Q_p(W_r)$. Eventually, the global flow rate (Q_g) is compared with those of the experiment for all the pressure tests, see in *Figure 17*, and shows a good agreement.

CONCLUSION

The simulation in this paper presents various results regarding the mechanical behaviour and the leak-tightness of the containment building with VERCORS mock-up. In mechanical part, early-age phase, prestress phase and pressurization phase are included. The vertical cracking patterns are firstly detected in the gusset because of the early-age effect. In prestress phase, the crack openings are partially closed, and are re-opened during the pressurization phase. The strains evolutions are extracted and are compared with those of the experiment, and the simulation estimates those strains in the same order as the results of the experiment. It is found that those strains are mainly contributed from prestress effect and delayed strains, thus the delayed strains should be estimated from the corresponding relative humidity. Besides that, the stresses in the wall are reduced in time evolution, and this is because of the increasing in prestress loss due to the delayed strains. Based on the mechanical results, leak-tightness in this paper is composed of porosity leakage and local through crack leakage. The post-processing of global flow rate shows that Q_g calculated from $Q_p(W_r)$ provides a good agreement to the results of the experiment.

REFERENCE

Bazant Z. P. and Yunping X. "Drying creep of concrete: constitutive model and new experiments separating its mechanisms". *Materials and Structures*. - 1994. - Vol. 27. - pp. 3-14.

BPEL99 "French design code for pre-stressed concrete, extended up to C80 in 1999".

Castem 2019 "User's guide". CEA-DES/DM2S/SEMT. - 2019. - http://www-cast3m.cea.fr/.

J. Niepceron "Benchmark VERCORS 2022: Prestressed concrete containment building". - 2021.

Jason L., Pijaudier Cabot G., Ghavamian S., Huerta A. "Hydraulic behaviour of a representative structural volume for containment buildings". *Nuclear Engineering and Design*, 2007. - Vol. 237.

Jason L. and Masson B. "Comparison between continuous and localized methods to evaluate the flow rate through containment concrete structures". *Nuclear Engineering and Design*, 2014. - Vol. 277.

Matallah M., La Borderie C. and Maurel O. "A practical method to estimate crack openings in concrete structures". *International Journal for Numerical and Analytical Methods in Geomechanics*, 2010. - 15 : Vol. 34.

Mazars J., Hamon F. and Grange S. "A new 3d damage model for concrete under monotonic, cyclic and dynamic loadings". *Materials and Structures*. - 2015. - Vol. 48. - pp. 3779-37793.

Wittmann F. and Roelfstra P. "Total deformation of loaded dring concrete". *Cement and Concrete Research*. - 1980. - 5 : Vol. 10. - pp. 601-610.